



E-ISSN: 2687-6167

Number 55, December 2023

RESEARCH ARTICLE

Receive Date: 02.12.2023

Accepted Date: 31.12.2023

# Synthesis and characterization of polymer-derived nanocrystal SiOC powders via high temperature XRD method

Sait Altun<sup>1\*</sup>, Hasan Göçmez<sup>2</sup>

<sup>1</sup>Kütahya Dumlupınar University, Advanced Technologies Center (İLTEM), ORCID: 0000-0003-3085-1351

<sup>2</sup>Kütahya Dumlupınar University, Faculty of Engineering, Department of Metallurgical and Materials Engineering, Kütahya, ORCID: 0000-0003-3748-0311

## Abstract

In the study, polymer-derived SiOC powders was synthesized by sol-gel method. The resulting composites consists of  $\beta$ -SiO<sub>2</sub>, SiC and free carbon. Tetraethylorthosilicate (TEOS) and Polydimethylsiloxane (PDMS) were selected as starting materials to obtain organic-inorganic structure. After the gelling process, the powders were heat treated at 1100°C in Argon medium to obtain the desired phases. Scanning Electron Microscopy (SEM), Differential Thermal Analysis (DTA) and Fourier Transform Infrared Spectroscopy (FT-IR) analyses were used for characterization. In addition, instant phase changes were determined by high-temperature XRD in powders subjected to heat treatment up to 1500 °C in a helium environment. The effect of temperatures on the transformation in SiOC synthesis, the transformation temperatures of  $\alpha$ -cristobalite to  $\beta$ -cristobalite were sharply determined and the SiC formation temperature was revealed. The effect of temperature on crystal size was also obtained as a result of the study.

© 2023 DPU All rights reserved.

Keywords: Polymer Derived Ceramics, SiOC, PDMS, High Temperature XRD

## 1. Introduction

Polymer derived ceramics (PDCs) are predominantly covalently bonded advanced ceramics that can be processed at relatively low temperatures such as 1000-1500 °C. The PDCs are obtained via polymer cross-linking and then a pyrolysis process in inert atmosphere. This is the process called polymer to ceramic conversion[1]. There are very large number of varieties of PDCs such as, SiC[2], SiOC[3], SiCN[4], SiBN[5] have been successfully synthesized using preceramic polymers as raw material.

PDCs are versatile material so they enable many applications such as sensors [6-7], coatings [8], high temperature structure material [9-10].

SiOC (black glass) is one of the most attractive materials in terms of optical, electrical and magnetic properties in recent years [11]. The high compositional stability and oxidation resistance and the superior properties in terms of mechanical and thermal properties are among the other features that make the usability of this material [12-14].

Silicon oxycarbide is called the structure in which silicones bond simultaneously with C and O atoms in the structure. This tetrahedral bond structure is usually define as [C<sub>x</sub>SiO<sub>4-x</sub>](x=1,2,3). The addition of carbon in silicate glass allows a coordination

<sup>1</sup> Corresponding author.

E-mail address: [sait.altun@dpu.edu.tr](mailto:sait.altun@dpu.edu.tr)

number of 4 to be obtained as a result of its replacement with oxygen, which has coordination number of 2. This increase in the number of bond per anion is expected to strengthen the chemical structure of glass lattice and also expected to improve thermal and mechanical properties. The sol-gel process enables the low-temperature synthesis of silicon oxycarbide glasses without problems such as oxidation during degradation and melting. What makes this process possible is the use of polymeric materials with Si-C bonds as starting materials [15].

The first findings about SiOC date back to 1989. Porte L. and Sarte A. investigated the effects of the reinforcement of silicon carbide materials in composite materials on high temperature behavior. The result of that study, the behavior of oxygen atoms was examined by XPS analysis and a small amount of SiO<sub>2</sub> phase was observed in the fiber material. In addition, the SiOC structure, which appears to be more abundant, was also determined [16].

In the study examining the pyrolysis steps of 400-1000°C, Babonneu et al. stated that the gel was stable at 400°C, decomposition started between 400-600°C and Si-O, Si-C bonds started to form, methyl groups were decomposed at 600-800°C and Si-C bonds were formed at 1000 C [17].

Chi. et al. reported that using TEOS and methyltrimethoxysilane (MTMS), the powder color turned black after the pyrolysis process in Argon medium at 1200°C, and proposed that crystalline phases were formed after 5 hours of heat treatment in Ar medium at 1450°C, and these phases were β-SiC and Cristobalite [18].

The aim of this study is to produce SiOC powders using PDMS/TEOS by the sol-gel method and to observe the phase changes instantly from 1100 to 1500 °C by using high temperature XRD.

## 2. Experimental Procedure

### 2.1. Synthesis of TEOS/PDMS Organic-Inorganic Hybrid Material

TEOS and PDMS were selected as the starting material for the Sol-Gel Method. Isopropyl alcohol (iPrOH) was used as the solvent of these two materials, nitric acid (HNO<sub>3</sub>) as the catalyst and purified water as the hydrolysis agent. TEOS and PDMS were determined as 60% TEOS and 40% PDMS by weight and the teos/iPrOH/H<sub>2</sub>O/HNO<sub>3</sub> molar ratio was adjusted in 5 different compositions as (1) 1:6: 3: 0.3 (25 °C), (2) 1: 6: 3: 0.6 (25 °C), (3) 1: 6: 3: 0.6 (50 °C), (4) 1:12: 3: 0.3 (25 °C), (5) 1: 15: 3:0.3 (25 °C) and duration of gelling time were controlled. The composition with the fastest gelation time was composition 3.

Composition 3 was used for the process referred to as organic-inorganic hybrid powder preparation. Two different solutions were prepared in two different beakers. (a) in the first beaker, half of the amount of TEOS, PDMS and total iPrOH to be used; (b) in the second beaker, the remaining iPrOH, H<sub>2</sub>O and HNO<sub>3</sub> were mixed until they were homogeneous solutions. Then, container b was slowly added to container a and continued to be stirred till it was homogeneous. The solution, which gelled at 50 °C in about 120 minutes, was left to dry until the weight loss was over.

Table 1. Gelation temperatures and times of the used composition.

Composition	Gelling Time	Gelling Temperature
1	1 day	25 °C
2	300 minutes	25 °C
3	120 minutes	50 °C
4	240 minutes	25 °C
5	240 minutes	25 °C

### 2.2. Preparation and sintering of SiOC powders

The hybrid material obtained was subjected to burning for 60 minutes at a heating rate of 5 C/min at 300 °C. This process has been carried out to avoid the free carbon content that may occur in the body. The light yellow brittle gel agate obtained was ground in the mortar until it passed completely under a 63 μm sieve. This hybrid material will be called raw powder in the article and all the heat treatments will be carried out on this raw material.

- I. The hybrid material obtained was subjected to heat treatment in Argon medium for 120 minutes at 1100 °C.

- II. The hybrid material was subjected to heat treatment in helium environment with a high-temperature XRD of 25 °C, 1100 °C, and after this temperature, an XRD pattern was determined every 50 °C with a heating rate of 5 °C/min.
- III. The hybrid material was subjected to heat treatment in a helium environment with a heating rate of 5 °C/min with its high-temperature XRD at 25 °C, 600 °C, after 120 minutes at 600 °C, 1000 °C, 1050 °C, 1100 °C, after 120 minutes at 1100 °C, and then right after this temperature XRD pattern was obtained every 50 °C.

Table 2. Heat treatment of organic-inorganic hybrid material.

Heat Treatment Steps	Precursor	Heat treatment temperature	Holding time	Heating Rate	Ambient Atmosphere
I	Composition 3	1100 °C	2hours at 600 °C and 2 hours at 1100 °C	5 °C /minutes	Argon
II	Composition 3	1500 °C	No holding	5 °C /minutes	Helium
III	Composition 3	1500 °C	2hours at 600 °C and 2 hours at 1100 °C	5 °C /minutes	Helium

### 2.3. Characterization processes

According to the high-temperature XRD results, it was determined that the SiO<sub>2</sub> and SiC phases in regime (iii) were more prominent, and the raw material of this sample was selected in the preheating analysis. XRD analysis was performed to determine the temperature-dependent phase transformations and crystal sizes of the powders. SEM (FE-SEM Fei Nanonova 650) and EDS analyses were conducted to examine the morphology of the raw and heat-treated material with chemical analysis. DTA-TG (STA 409 PC) analysis was executed to determine possible reaction temperatures and weight loss. FT-IR analysis was performed to determine the bond structures in glassy regions.

### 3. Results

According to Figure 1, in the FTIR analysis of the raw powder, Si-O bonds at 559 cm<sup>-1</sup> and 699 cm<sup>-1</sup>, C≡CH bonds at 455 cm<sup>-1</sup>, CO-OH bonds at 1402 cm<sup>-1</sup> and C-CH<sub>3</sub> bonds at 2962 cm<sup>-1</sup> are observed [19]. Si-C bonds are seen at 787 cm<sup>-1</sup> and 853 cm<sup>-1</sup> wavelengths, Si-O-Si at 1008 cm<sup>-1</sup> and Si-CH<sub>3</sub> bonds at 1258 cm<sup>-1</sup> [20]. In the sample obtained after high-temperature XRD, Si-O-Si bonds at 1085 cm<sup>-1</sup> and Si-C bonds at 668 cm<sup>-1</sup> and 792 cm<sup>-1</sup> are clearly seen in the structure [21,22]. In addition, in the C-H and CH<sub>3</sub> bonds in the structure were reduced.

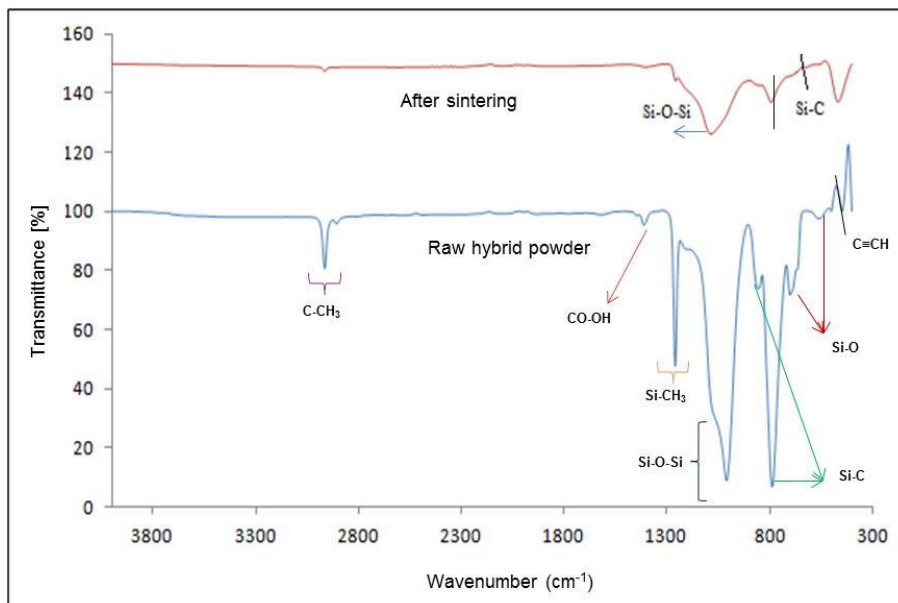


Fig. 1. FT-IR analysis of hybrid powder after raw and heat treatment.

In the phase analysis determination performed before and after the heat treatment, it was observed that the raw state of the produced organic-inorganic hybrid powder was amorphous according to the XRD result, and no crystalline structure peak was formed. The peaks seen in the XRD pattern are derived from the platinum substrate used for the high-temperature XRD (Figure 2.). The diffraction peaks corresponding to  $\alpha$ -cristobalite (Highscore: 98-016-2245),  $\beta$ -cristobalite( Highscore:98-016-2666) and SiC (Highscore: 98-018-2362) (Figure 4 and Figure 5.).

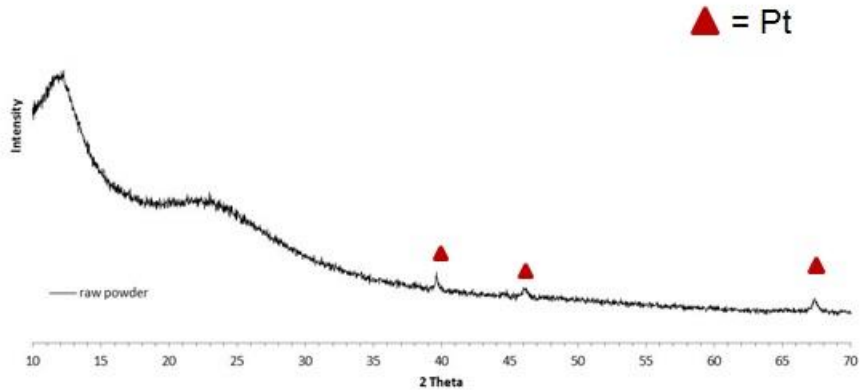


Fig. 2. XRD pattern of raw hybrid material.

The raw powder obtained was subjected to a pyrolysis process in an argon environment at 1100 °C for 2 hours at the first stage. It was observed that the obtained structure preserved its amorphous structure while the  $\alpha$ -cristalloid phase started to form (Figure 3.).

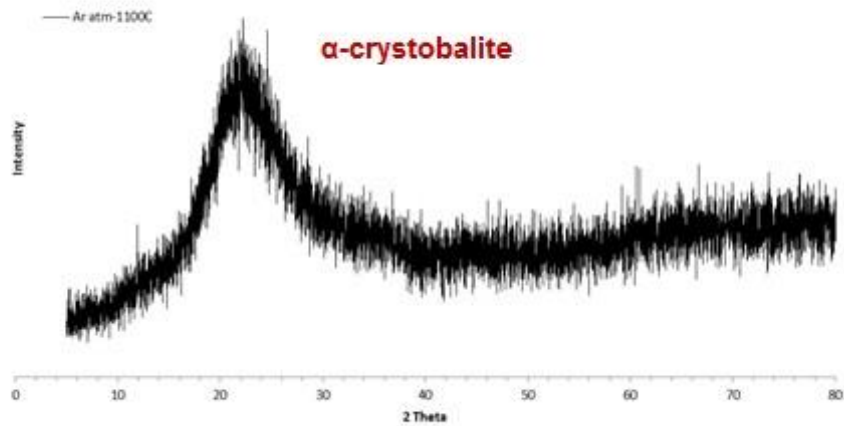


Fig. 3. XRD graph of the sample subjected to pyrolysis at 1100 °C in Ar medium.

For the high-temperature XRD analysis to observe phase transformations, heat treatment steps up to 1500 °C were carried out at annealing and pyrolysis critical temperatures ( 600 °C and 1100 °C) without waiting certain time and holding for 2 hours at both temperatures (Figure 4 and Figure 5).

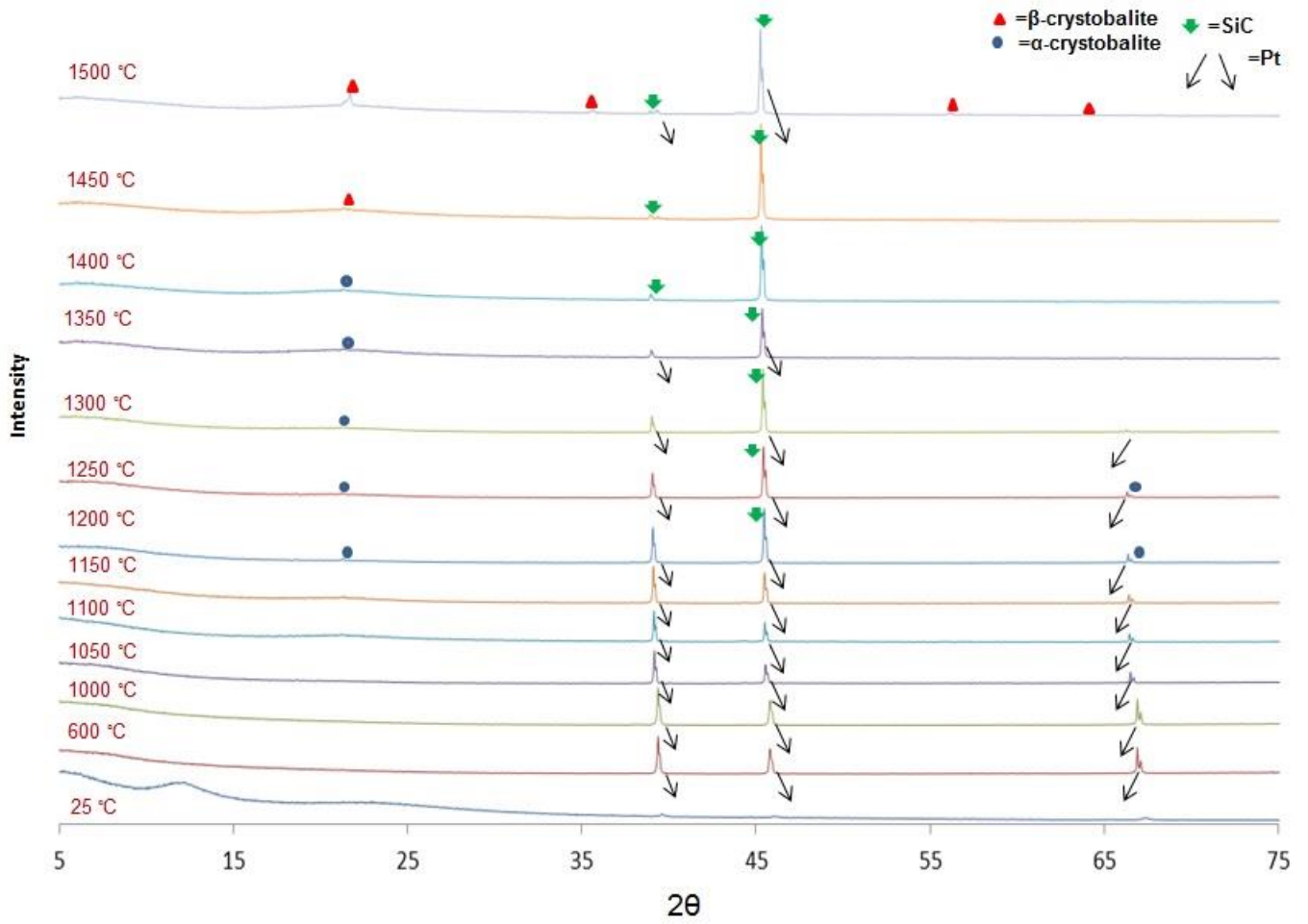


Fig. 4. High temperature XRD patterns (no holding time at annealing and pyrolysis temperature)

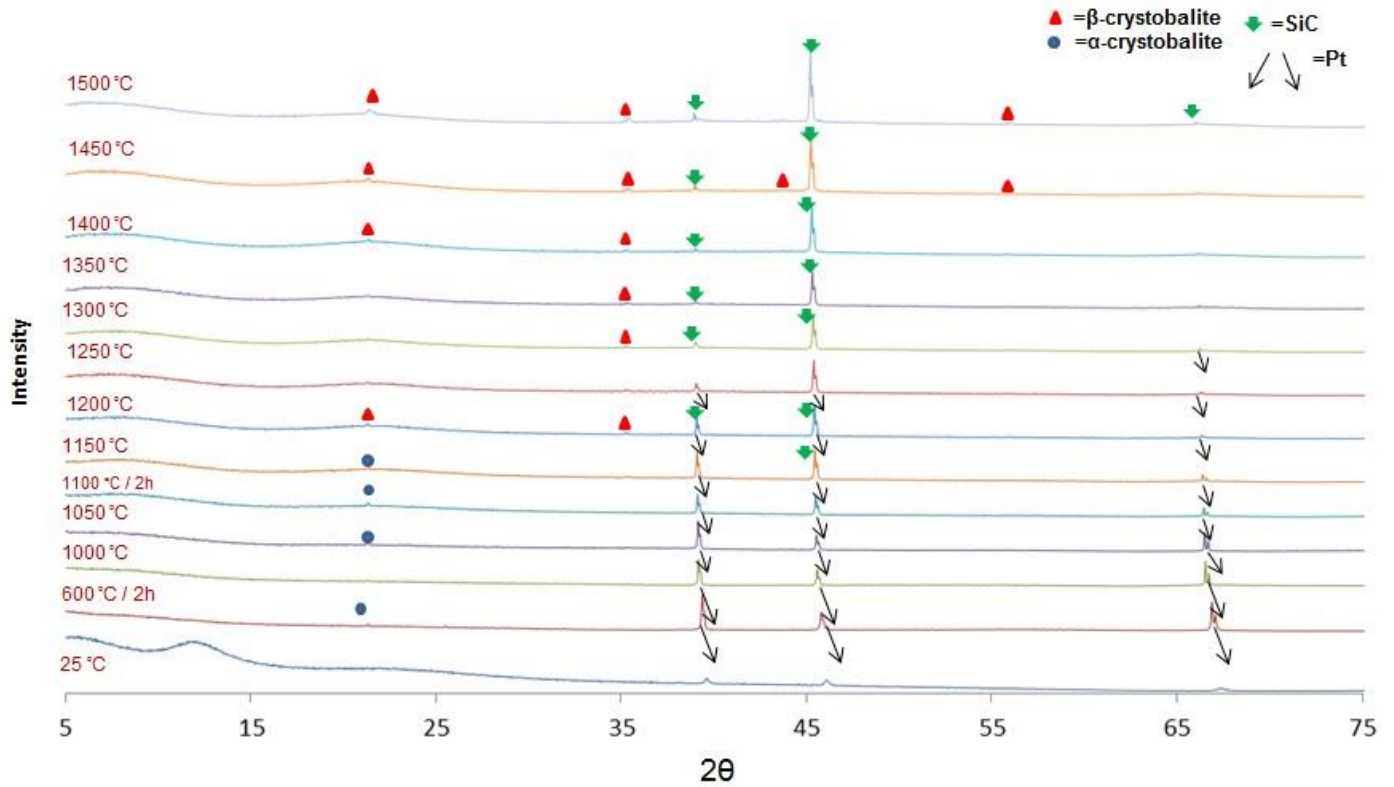


Fig. 5. High-temperature XRD patterns (Sample holding for 2 hours at annealing and pyrolysis temperature)

According to Figure 4, it was observed that  $\alpha$ -cristobalite peaks were formed at 1200 °C- 1400 °C, and the structure transformed into the  $\beta$ -cristobalite phase after 1450 °C. In addition, it was detected that SiC peaks started to form in the structure around 1250, then this phase was clarified at above 1450 °C.

According to Figure 5, it was observed that there is an  $\alpha$ -crystalloid phase in the structure starting from 600 °C. It turns into a  $\beta$ -crystalloid phase at 1200 °C, the phase disappears with the increase in temperature, and it occurs again at 1400-1450 °C. For the SiC phase, it was perceived that the first peaks started to be seen at 1150-1200 °C, but became clear at 1450 °C and were completely found at 1500 °C.

According to both Figure 4 and Figure 5, It's seen that there is no SiC peak in the structure up to 1100 °C. In Figure 4, it was observed that SiC peaks were formed at 1200 °C and these peaks become more pronounced as the temperature increases. In Figure 5, it was seen that the SiC formation temperature decreased to 1150 °C. It can be said that holding at critical temperatures during the heat treatment reduces SiC formation to lower temperatures.

As a result of the heat treatment, it was observed that the initial amorphous structure turned into a crystal structure as the temperature increased, but the amorphous separation in the structure remained in the system. The crystal sizes of the SiO<sub>2</sub> and SiC phases, which are among the crystalline structures formed, are given in Table 3 and Table 4.

Table 3. Crystal size change of the sample at annealing and pyrolysis temperature without holding times.

Temperature (°C)	SiO <sub>2</sub> (nm)	SiC(nm)
1000	-	-
1050	-	-
1100	30.3	-
1150	65.3	-
1200	65.4	-
1250	46.9	-
1300	30.3	-
1350	47	-
1400	65.3	-
1450	65.3	226
1500	82.4	454

Table 4. Crystal size change of the sample at annealing and pyrolysis temperature with 2 hours holding times.

Temperature (°C)	SiO <sub>2</sub> (nm)	SiC(nm)
1000	-	-
1050	-	-
1100	218	-
1150	114	-
1200	218.2	-
1250	218.5	-
1300	-	-
1350	11.1	-
1400	65.3	-
1450	114	69
1500	218.2	120

According to the results obtained, the increase in heat treatment time led to the formation of SiC crystals in larger sizes. Depending on the temperature, crystal size growth is also seen in the results as expected.

The prepared hybrid material was subjected to DTA-TG analysis in such a way that annealing and pyrolysis temperatures up to 1500 °C were kept for 2 hours in Argon medium (Figure 6.).

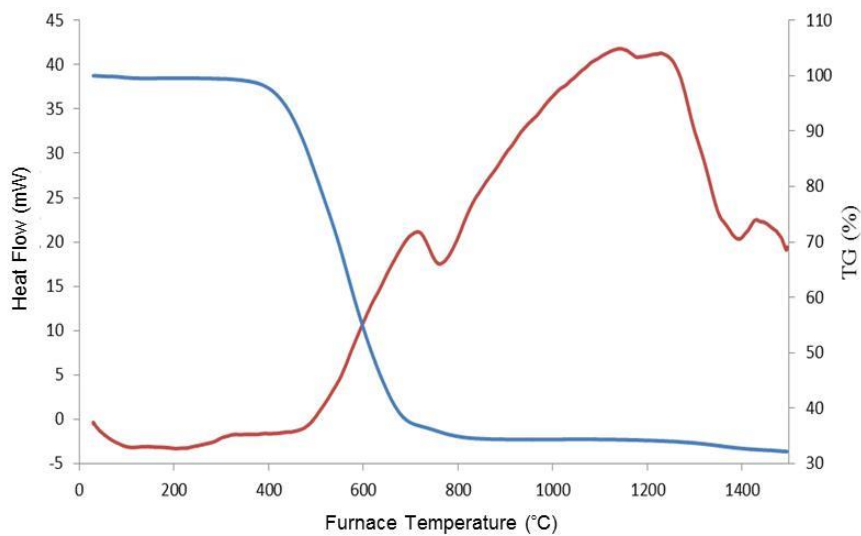


Fig. 6. DTA-TG analysis of hybrid powder up to 1500 °C

According to the results of the analysis, it was observed that weight loss occurred due to decomposition reactions between 400-800 °C. It was supported by the XRD result that the exothermic reaction at 1100 °C is the SiO<sub>2</sub> formation reaction and the exothermic reaction at 1400 °C is the SiC phase formation reaction.

According to the SEM analysis performed on the raw powder, it is seen that the structure is completely amorphous. EDX analysis was performed to determine the elemental constitution in the structure (Figure 7, Figure 8 and Table 3).

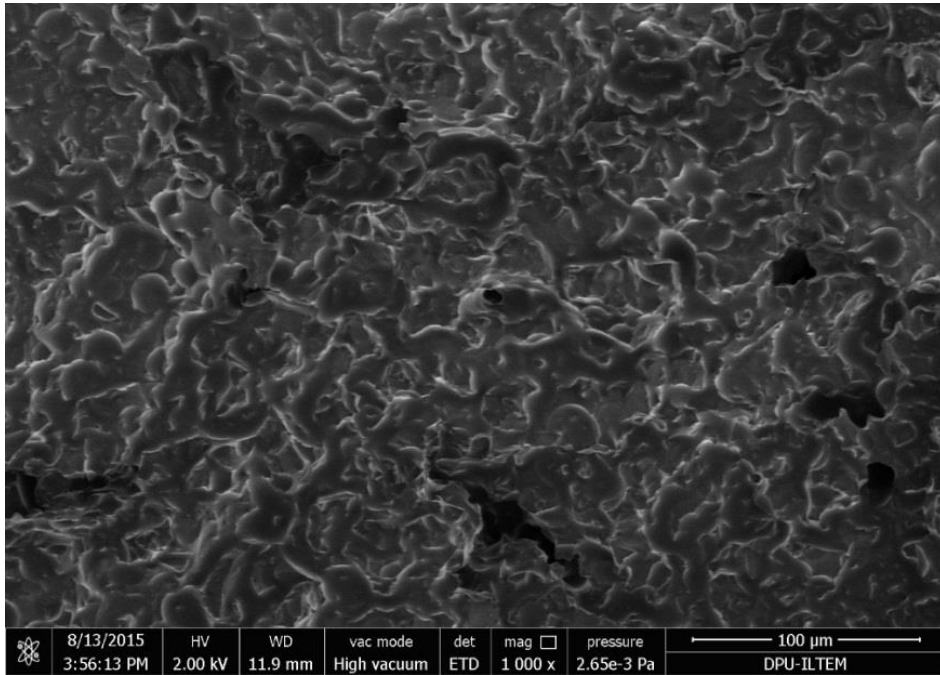


Fig. 7. SEM image of raw powder.

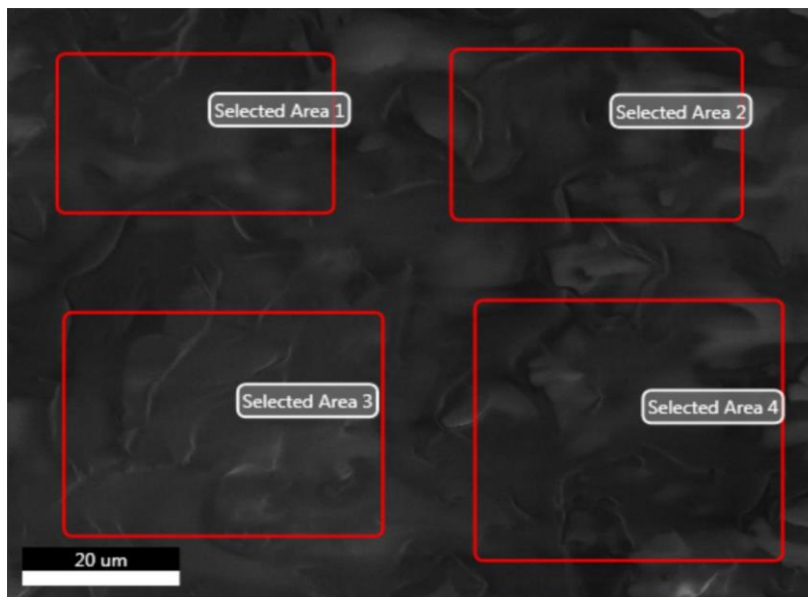
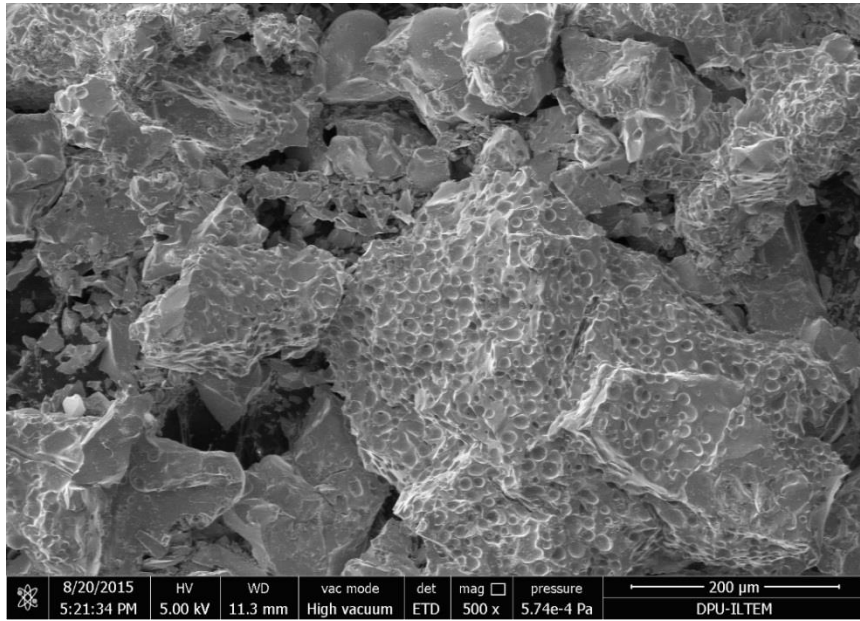


Fig. 8. EDX analysis of raw powder.

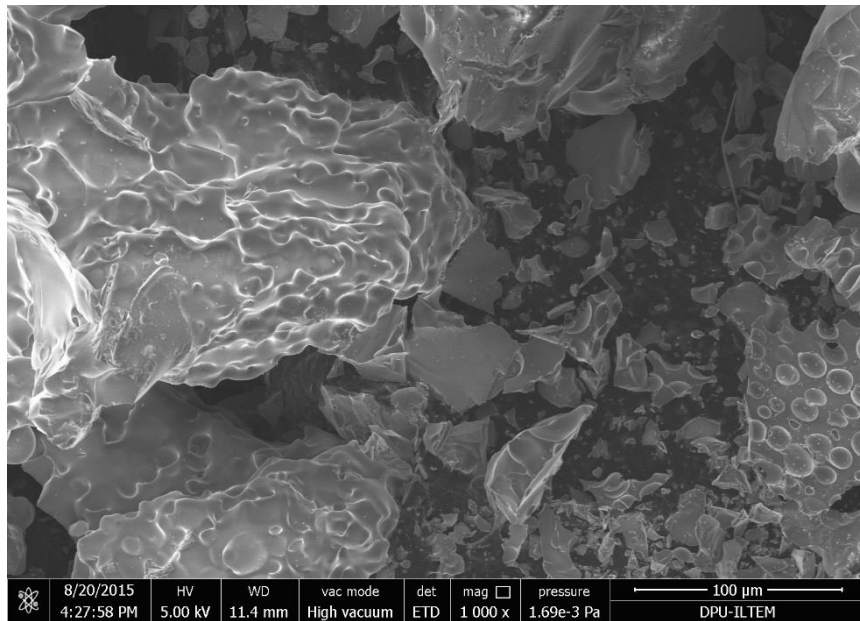
Table 3. Average EDX analysis of raw powder.

Element	By Weight (%)	atomic
Si	35.7	21.3
O	21.3	21.3
C	41.3	57.4

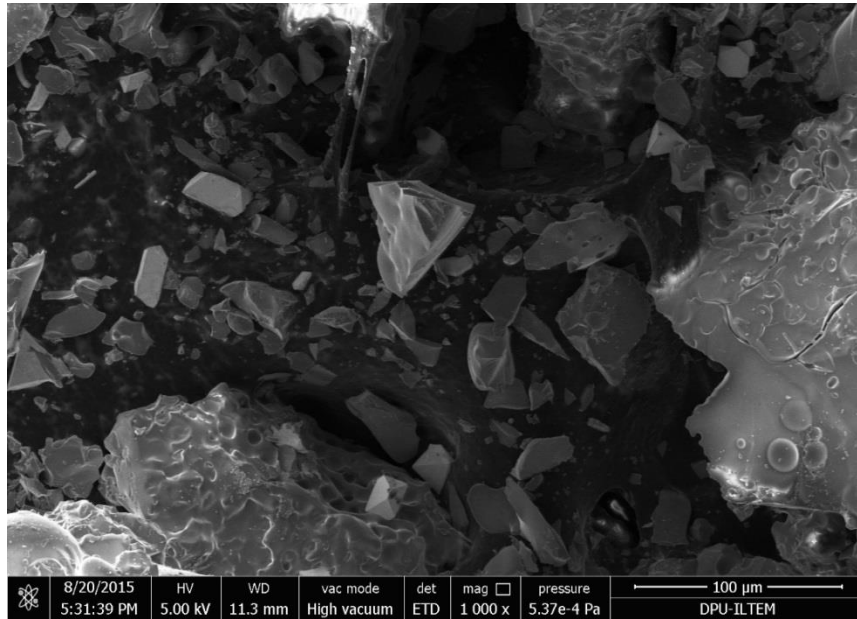
The SEM results of the sample subjected to heat treatment with high-temperature XRD are given in Figure 9.



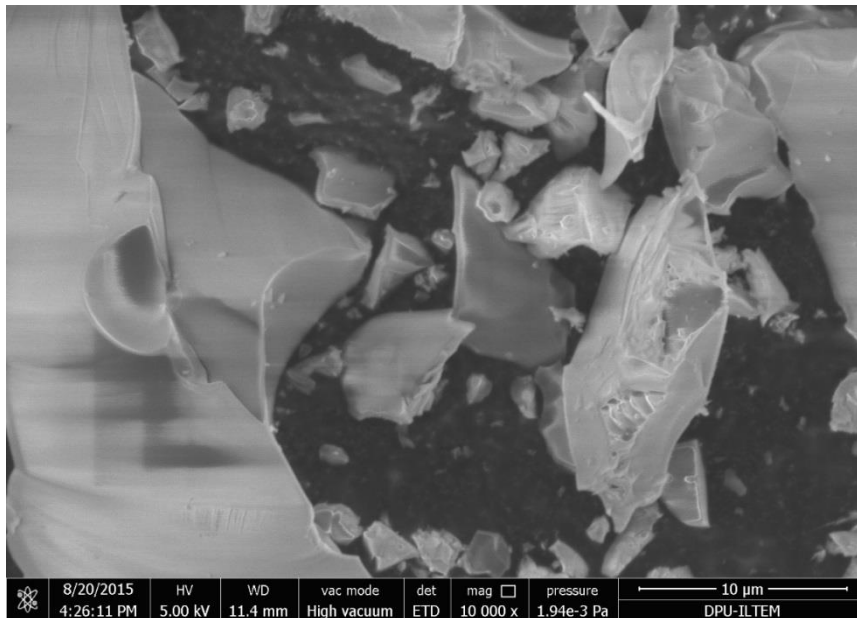
(a)



(b)



(c)



(d)

Fig. 9. SEM analysis of sample heat treated with high-temperature XRD (Sample holding for 2 hours at annealing(600 °C) and pyrolysis( 1100 °C) temperature) a) 500X, b) 1000X, c) 5000X d) 10000X.

The amorphous composition in the morphology with the presence of crystalline structure were observed at the same time, and it was determined that porous structures were also present (Figure 9). As expected in the heat-treated sample, the decrease of C and O atoms was also revealed according to the EDX analysis (Figure 10 and Table 4.) [23].

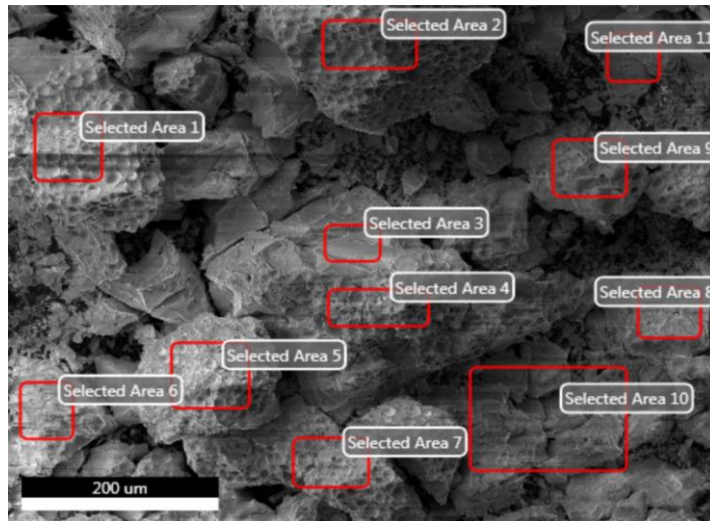


Fig. 10. EDX image of the heat-treated sample.

Table 4. Average EDX analysis of the heat-treated sample.

Element	By Weight (%)	atomic
Si	38,4	25,62
O	55,5	64,9
C	6	9,35

#### 4. Conclusions

It has been observed that the polymer-derived sol gel method is a successful method for SiOC production. In particular, High temperature XRD was of great benefit to see how the structure changes with temperature. In the compositions prepared for organic-inorganic hybrid powder synthesis, it was observed that only increasing the solvent ratio had no effect on gelation. While the hybrid structure, which is the raw material of SiOC powder, is completely amorphous at room temperature it's seen from XRD and SEM result that the structure turns into a crystalline structure at 1500 °C. In this composition where the crystalline and amorphous structures coexist FT-IR analysis was used to investigate the bond structures and Si-O-Si and Si-C bonds were determined. It has been determined that the sintering regime has an effect on the microstructure, and it has been revealed that it has profound effects on phase formations and crystal size. Phase conversion reaction temperatures were determined in the base of XRD and DTA analysis results. The differences in the C and O atoms between the raw sample and the heat-treated sample were determined by EDX analysis.

#### Acknowledgment

This study is derived from the author's master's thesis on the Synthesis and Characterization of Polymer Derived Nanocrystalline SiOC Powders. We would like to thank Kütahya Dumlupınar University Advanced Technologies Center and analysis supervisors for their great help in carrying out the analyses used in experimental studies.

#### References

- [1] L, Jingjie., D, Qingwen., Y, C., Giuntini, D., & R. Riedel., (2023). Preparation of polymer-derived SiOC-Cu ceramic composites and their tribological performance, *Journal of the European Ceramic Society*, (in-press article).
- [2] Y. J. Shim., S. H. Joo., H. J. Lee., K. W. Cho., & Y. J. Joo., (2023). The effect of temperature and atmospheric-pressure on mechanical and electrical properties of polymer-derived SiC fibers. *Oper Ceramics*, 15, 100431.
- [3] G. J. Leonel., X. Guo., G. Singh., & A. Navrotsky., (2023). Chemistry, structure and thermodynamic stabilization of SiOC polymer derived ceramics made from commercial precursor. *Open Ceramics*, 15, 100402.
- [4] K. Liu., W. Peng., D. Han., Y. Liang., B. Fan., H. Lu., H. Wang., H. Xu., R. Zhang., & G. Shao., (2023) Enhanced piezoresistivity of polymer-derived SiCN ceramics by regulating divinylbenzene-induced free carbon. *Ceramics International*, 49, 2296-2301.
- [5] Y. Liu., K. Chen., F. Dong., S. Peng., Y. Cui., C. Zhang., K. Han., M. Yu., & H. Zhang., (2018). Effects of hydrolysis of precursor on the structure and properties of polymer-derived SiBN ceramic fibers. *Ceramics International*, 44, 10199-10203.

- [6] Z, C., X, Chen., X, Li., & G, S., (2023). Thin-film temperature sensor made from polymer-derived ceramics based on laser pyrolysis. *Sensors and Actuators: A. Physical*, 350, 114144.
- [7] Q, Yan., S, Chen., H, Shi., X, Wang., S, Meng., & J, Li., (2023). Fabrication of polymer-derived SiBCN ceramic temperature sensor with excellent sensing performance. *Journal of the European Ceramic Society*, 43, 7373-7380.
- [8] X, Zhang., y, Zhang., L, Gou., B, Liu., Y, Wang., H, Li., H, Li., & J, Sun., (2024). Ablation resistance of ZrC coating modified by polymer-derived SiHfOC ceramic microspheres at ultrahigh temperature. *Journal of Materials Science & Technology*, 182, 119-131.
- [9] Z, Li., & Y, Wang., (2017). Preparation of polymer-derived graphene-like carbon-silicon carbide nanocomposites as electromagnetic interference shielding material for high temperature applications. *Journal of Alloys and Compounds*, 709, 313-321.
- [10] Y, Lu., Y, Sun., T, Zhang., F, Chen., L, Ye., & T, Zhao., (2019). Polymer-derived Ta<sub>4</sub>HfC<sub>3</sub> nanoscale ultrahigh-temperature ceramics: Synthesis, microstructure and properties. *Journal of the European Ceramic Society*, 39, 205-211.
- [11] M. A. Mazo, A. Nistal, A.C. Caballero, F. Rubio, J. Rubio, J.L. Oteo, (2013), Influence of processing conditions in TEOS/PDMS derived silicon oxycarbide materials. Part 1: Microstructure and properties *Journal of the European Ceramic Society* 33, 1195-1205.
- [12] A. Kloneczynski, R. Riedel, G. Mera and R. Hauser, (2006), " Silicon-Based Polymer-Derived Ceramics: Synthesis Properties and Applications-A Review, *Journal of the Ceramic Society of Japan* 114 (6), 425-444.
- [13] P. Colombo, (2010), " Polymer-Derived Ceramics: 40 Years of Research and Innovation in Advanced Ceramics' ", *Journal of American Ceramic Society*, 93 (7), 1805-1837
- [14] E. Bernardo, L. Fiocco, G. Parciannello, E. Storti, P. Colombo, (2014), "Advanced Ceramics from Pre ceramic Polymers Modified at the Nanoscale: A Review" *Materials*, 7, 1927-1956
- [15] H. Zhang, C. G. Pantano, A. K. Singh, (1999), Silicon Oxycarbide Glasses, *Journal of Sol-Gel Science and Technology*, 14, 7-25
- [16] Porte, L. & Sarte, A. (1989), Evidence for a silicon oxycarbide phase in the Nicalon silicon carbide fibre: *Journal of Materials Science* cilt 24 s.271-275.
- [17] F. Babonneau, L. Bois and J. Livage, (1992), Silicon oxycarbides via sol-gel route: characterization of the pyrolysis process *Journal of Non-Crystalline Solids* 147-148, 280-284
- [18] F. K. Chi, (1983) " Carbon-Containing Monolithic Glasses via the Sol-Gel Process' " *Ceram. Eng. Sci. Proc.* 4, 704-717
- [19] J. Rumble, (Ed.). (2017). *CRC handbook of chemistry and physics*.
- [20] Y-L. Li, D. Su, H-J. An, X. Liu, F. Hou, J-Y. Li, X. Fu, (2010), Pyrolytic transformation of liquid precursors to shaped bulk ceramics, *Journal of European Ceramic Society*, 30, 1503-1511
- [21] X. Wang, J. Qian, C. He, A. Shui, B. Du, (2023), The structural evolutions and enhanced thermal stability of Al cation-modified silicon oxycarbide ceramics, *Journal of Sol-Gel Science and Technology*, 106, 616-625
- [22] D-S. Ruan, Y-L. Li, L. Wang, D. Su, F. Hou, (2010), Fabrication of silicon oxycarbide fibers from alkoxide solutions along the sol-gel process, *Journal of Sol-Gel Science and Technology*, 56, 184-190
- [23] H, Tang., K, Wang., K, Ren., & Y, Wang., (2023). Microstructural evolution and microwave transmission/absorption transition in polymer-derived SiOC ceramics. *Ceramics International*, 49, 20406-20418.